

Supporting Information for:

Electrochemical Scanning Tunnelling Spectroscopy of a Ferrocene-modified n-Si(111) - Surface: Electrolyte Gating and Ambipolar FET Behaviour

Artem Mishchenko^a, Mufida Abdulla^b, Alexander Rudnev^{a,c}, Yongchun Fu^a, Andrew R. Pike^b and Thomas Wandlowski^a

^a Dept. Chem. Biochem., University of Bern, Freiestrasse 3, Bern, Switzerland. Fax: +41 31 631 3994; Tel: +41 31 631 5384; E-mail: thomas.wandlowski@dcb.unibe.ch

^b School of Chemistry, Newcastle University, Newcastle upon Tyne, UK. Fax+44 191 222 6929; Tel: +44 191 222 7061; E-mail: a.r.pike@ncl.ac.uk

^c A.N. Frumkin Institute of Physical Chemistry and Electrochemistry, Russian Academy of Sciences, Leninskii pr. 31, Moscow 119991, Russia

Materials and Methods

Vinyl ferrocene (97%) and 1-octene (98%) were purchased from Sigma Aldrich and used as received. Toluene was also purchased from Sigma Aldrich (ACS spectrophotometric grade, $\geq 99.5\%$), and was distilled over sodium prior to use. The n-type (phosphorous doped) silicon wafers, all <111> orientation with a miscut ranging between 0.1° and a resistivity of 1–10 $\Omega\text{-cm}$, were purchased from Compart Technology Ltd. (Peterborough, Cambridgeshire, United Kingdom).

1. Preparation of modified Si-surfaces, VFC and OCT

The following steps were performed to produce flat and clean modified silicon electrodes:^{1,2}

i) Silicon surface cleaning

The Si <111> orientated, low miscut angle wafer was cut into small squares of ca. 1 cm². These were cleaned by trichloroethylene (TCE, Sigma Aldrich, semiconductor grade) by boiling vigorously for 20 min. The chips were subsequently transferred to a vial containing acetone (Sigma Aldrich, semiconductor grade) and soaked at room temperature for 5 min. This procedure was repeated with 2-propanol (Sigma Aldrich, semiconductor grade) and a soaking time of 5 min. Finally, the sample was transferred to Nanopure water and soaked therein for 5 min.

ii) Preparation of uniform oxide layers:

The chips were transferred from Nanopure water into a freshly prepared piranha solution (1:4) (2 ml 30% H₂O₂, Sigma Aldrich, *TraceSELECT*[®], and 8 ml 96% H₂SO₄, Sigma Aldrich, semiconductor grade) and kept there for 20 min. The preparation of the piranha solution is an exothermic reaction, and heat is evolved. However, upon cooling down, the chip-containing solution was heated gently on a hotplate.

The chips were rinsed thoroughly with Nanopure water, and then stored in fresh Nanopure water until etching.

iii) Wet etching:

A home-built Teflon cell and plunger were rinsed thoroughly with Nanopure water to remove impurities. The trough was then half-filled with aqueous ammonium fluoride solution (Fluka, purum 40% in H₂O), and the chips were placed in a holder with the plunger raised so that the chips are seated at the top of the cell. The chips are mounted in such a way that the polished side is facing inwards in a vertical position. The cell lid was then screwed down securely, and an argon flow was introduced into the ammonium fluoride solution for 1 - 2 h.

Then the argon inlet line was lifted out of the solution to create an argon blanket above the cell before the plunger is pressed down to lower the chips into the deoxygenated ammonium fluoride solution to etch for 20-25 min. The chips were lifted out of the etching solution by raising the plunger and rinsed thoroughly with Nanopure water to remove any ammonium fluoride. Finally, any excess water was removed by placing the chip edges onto dry filter paper and blowing under a gentle stream of nitrogen, before they are quickly transferred to the appropriate reflux solution.

iv) Thermal alkylation:

The chips were alkylated in 20 mM of vinylferrocene in 10 ml dry toluene resulting in a VFC-modified Si(111) surface (**Fig. S1**), or in 20 mM of octene dissolved in 10 ml dry toluene, which leads to OCT-modified Si(111) samples (Fig. S1).

The chips were left to alkylate in these solutions overnight at reflux temperature under a nitrogen atmosphere. After reflux, the solution was allowed to cool, and the chips were removed under a positive pressure of nitrogen, rinsed with TCE and acetone (Sigma Aldrich, both semiconductor grade).

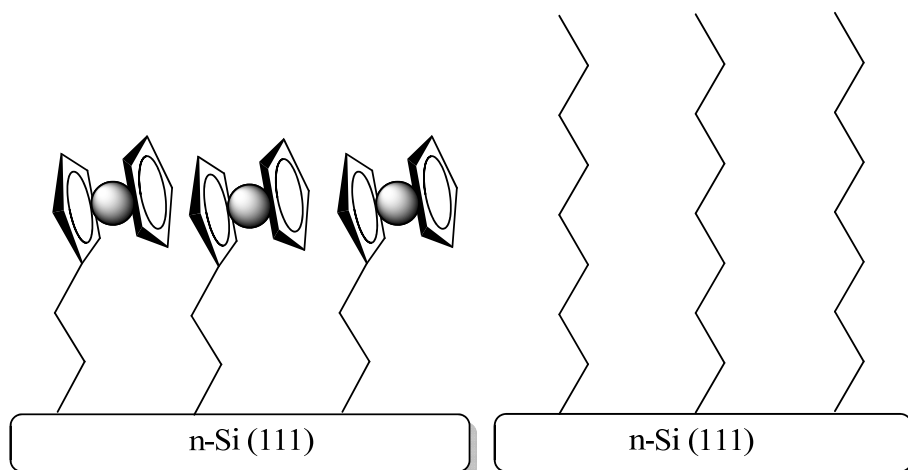


Fig. S1: VFC-modified Si(111) surface (left) and OCT-modified Si(111) surface (right).

2. Sample characterization

The tethered n-Si(111) samples were characterized by cyclic voltammetry (CV), *in situ* scanning tunnelling microscopy (STM) and ex situ atomic force microscopy (AFM). The STM measurements were carried out with a Molecular Imaging Pico-SPM. Details of experimental setup and procedures can be found elsewhere.^{3,4} In short, a small Kel-F cell (0.2 ml) was fixed on top of the modified Si substrate with a Kalrez O-ring attached to it. Electrochemical measurements were carried out in all-glass three-electrode cell with Autolab PGSTAT3. A palladium wire (0.5 mm diameter, saturated with molecular hydrogen (Pd-H)) was used as reference electrode, a platinum wire (0.5 mm diameter) served as counter electrode, and aqueous 0.1 M HClO₄ was chosen as supporting electrolyte. All CVs and *in situ* STM measurements were performed under argon. The STM tips were electrochemically etched from gold wires (0.25 mm) and coated with hot melt adhesive (Henkel, the major compound is ethylene vinyl acetate). The AFM images were recorded with a Nanosurf[®] EasyScan 2 FlexAFM in non-contact mode using standard n⁺-Si cantilevers (Nanosensors[™], resonance frequency 0.15-0.3 MHz, spring constant 20-80 N/m) under ambient conditions.

3. Cyclic voltammetry of VFC-modified Si(111) samples

Here we summarize the main results of a series of voltammetric measurements on n-Si(111) samples with various VFC coverages (0.035 (1%), 0.30 (6,7%), 0.54 (12 %) and 1.3 10⁻¹⁰ mol cm⁻² (29%)).

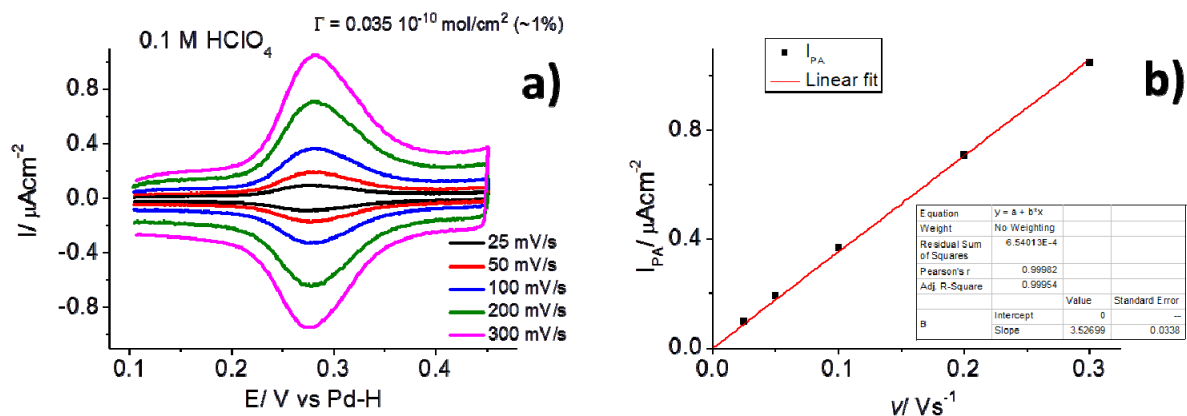


Fig. S2: (a) Cyclic voltammograms of VFC-modified Si(111) surface (small coverage). (b) Anodic peak height as a function of scan rate.

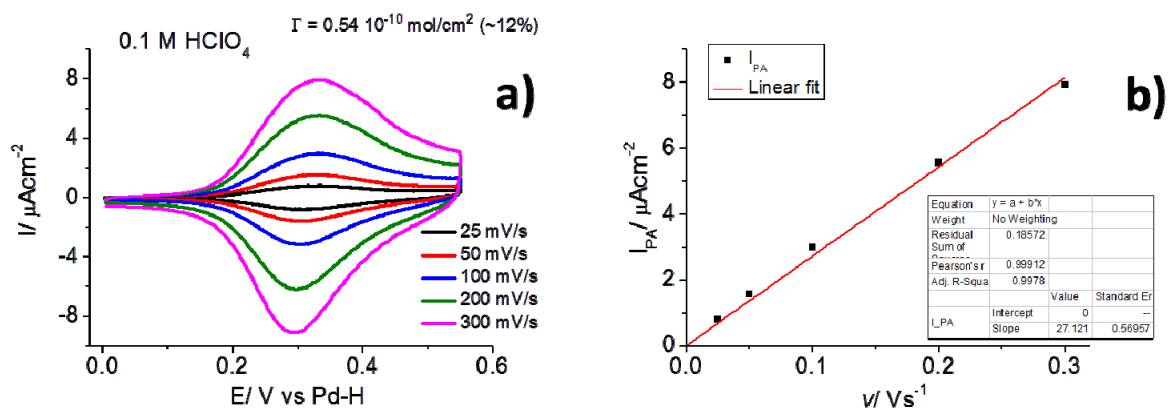


Fig. S3: (a) Cyclic voltammograms of VFC-modified Si(111) surface (medium coverage). (b) Anodic peak height as a function of scan rate.

Figs. S2 and S3 demonstrate, as examples of the above series, linear dependencies of the heights of the ferrocene redox peaks vs. the scan rate, which clearly represent a surface-confined redox process. In other words, the reductive (Fc) and oxidative (Fc⁺) forms of VFC are adsorbed and chemically bound on the electrode surface. **Fig. S4a** shows the comparison of cyclic voltammograms recorded for n-Si(111) samples modified with VFC of different coverage at 100 mVs⁻¹ (similar trends were observed for the entire range of scan rates investigated). Both the formal potentials as well as the peak-to-peak separations increase linearly with an increase of the VFC coverage. The concentration-dependent shift of the formal potential is attributed to the

doping of the n-Si(111) surface by the surface-immobilized Fc moieties. The increase in the peak-to-peak separation, which is paralleled by an increase of the FWHM of the anodic and cathodic redox peaks, is most probably related to repulsive lateral interactions within the VFC adlayer, which is stronger with higher adlayer coverage. We also notice that the shape of the anodic and cathodic redox peaks changes from a nearly ideal Langmuir-type appearance at low coverages (**Fig. S2** for $0.035 \cdot 10^{-10} \text{ mol cm}^{-2}$ (1%)) to a more distorted form at higher VFC coverages (**Fig. S4** and Fig. 1a in the main text). Deviations at higher coverages are attributed to the heterogeneity of the local environment around the ferrocene species and to dominating repulsive interactions. Nevertheless, we could extract, based on the peak-to-peak separation, which approaches exponentially to zero in the limit of zero scan rate, the standard rate constants k_s for the electron transfer applying Laviron's approach. **Fig. 4c** shows that k_s decreases with increasing VFC coverage. The dependence of k_s vs coverage is close to a hyperbolic (reciprocal) function. The peak-to-peak separations ΔE increase linearly with coverage (as shown in **Fig.4b**), and for peak-to-peak separations less than 60 mV the dependence of k_s vs ΔE is reciprocal as predicted for an ideal, Laviron-type surface-confined redox system.⁵

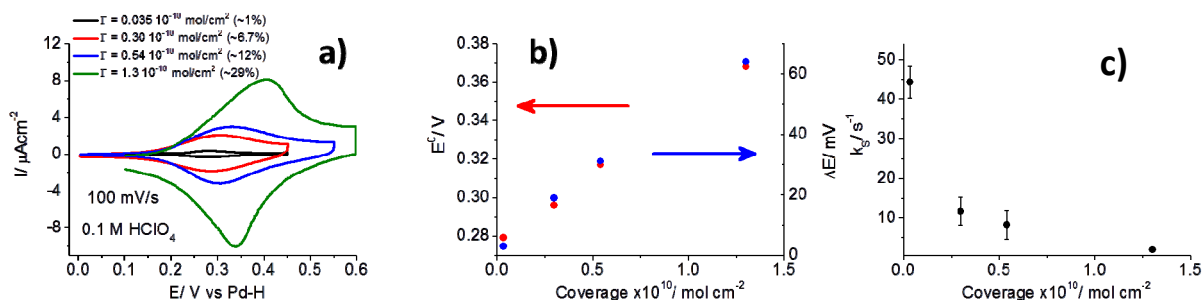


Fig. S4: (a) Comparison of cyclic voltammograms for different coverages of VFC on Si(111) surfaces. (b) Formal potentials E^0 and peak-to-peak separations ΔE at 100 mV s^{-1} as functions of the VFC coverage. (c) Standard rate constant k_s for the electron transfer estimated by applying Laviron's analysis, as a function of VFC coverage.

We also explored the effect of irradiation by white light on the electrochemical response of the n-doped silicon surface. Photons with an energy higher than the band gap (usually, even infrared radiation at 1100 nm is sufficient) hit the n-doped silicon surface, and create electron-hole pairs, which are required to promote the electro-oxidation of ferrocene. We found this phenomenon when comparing the CV responses obtained in the dark and under illumination. However, the effects were not as pronounced as reported in previous studies.^{6,7} We notice further, that we did not find any effect of silicon surface illumination on STM and STS responses in the present

study. We hypothesize that the doping level and the proximity of ferrocene to the surface are possible reasons for this behaviour. There is no photoeffect on the redox behaviour of ferrocene immobilized on heavily doped n-Si samples with a resistivity of the order of a few $\text{m}\Omega\cdot\text{cm}$ and short alkyl spacers ($< 0.4 \text{ nm}$).⁸ In contrast, moderately doped n-Si sample ($1\text{-}5 \Omega\cdot\text{cm}$) with long ferrocene spacers (ca. 1.5 nm long) behave for the redox response of ferrocene as insulators in the dark.⁶ Taking into account that our Si wafers have a very similar characteristics to those studied by Hauquier et al,⁶ but differ considerably in their response to illumination, we propose that the short $-\text{C}_2-$ linkers allow the ferrocene moiety a significant doping of the silicon surface, thus partially masking the photoeffect.

4. *In situ* scanning tunnelling microscopy (STM)

For comparison, STM images of OCT-modified and VFC-modified Si(111) surfaces are presented in **Fig. S5**. They were recorded under identical conditions. Clearly, no systematic change in the surface morphology is observed in the potential range between $0 \rightarrow 0.7 \rightarrow 0 \text{ V} \rightarrow 0 \text{ V}$ during imaging of the OCT sample (**Fig. S5a**), which is distinctly different for the VFC-modified samples (**Fig. 1c** in the main text and **Fig. S5b**).

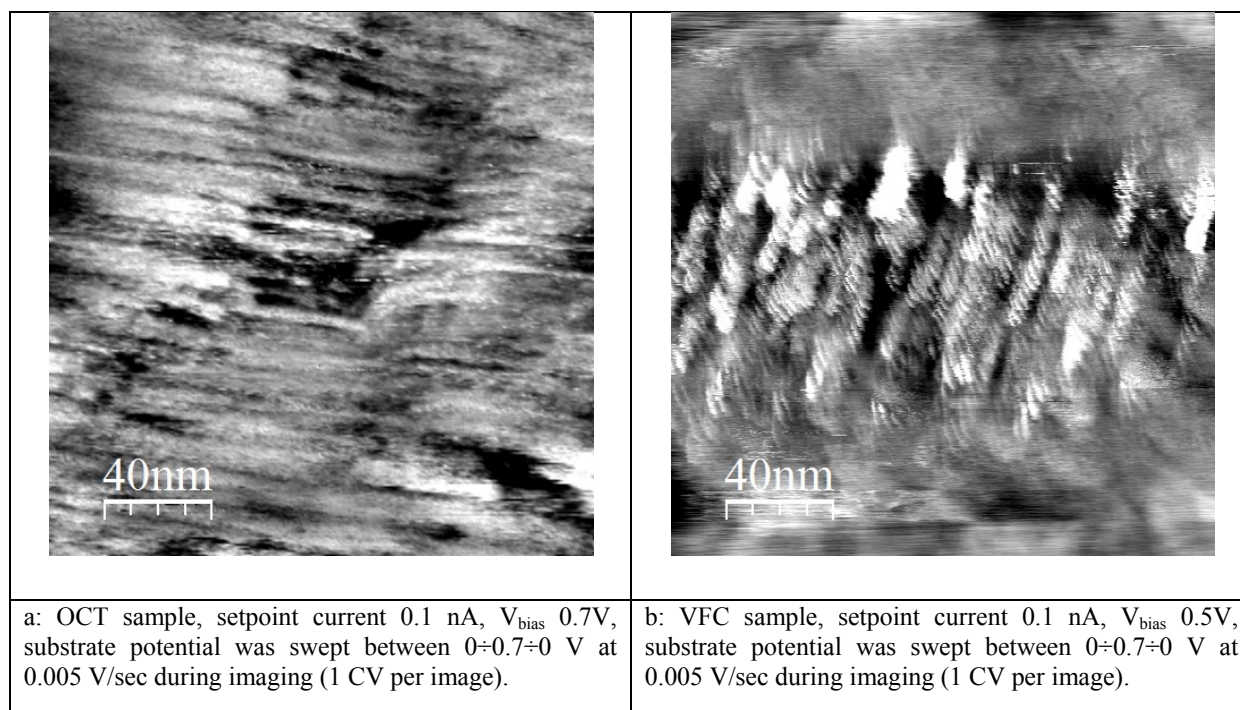
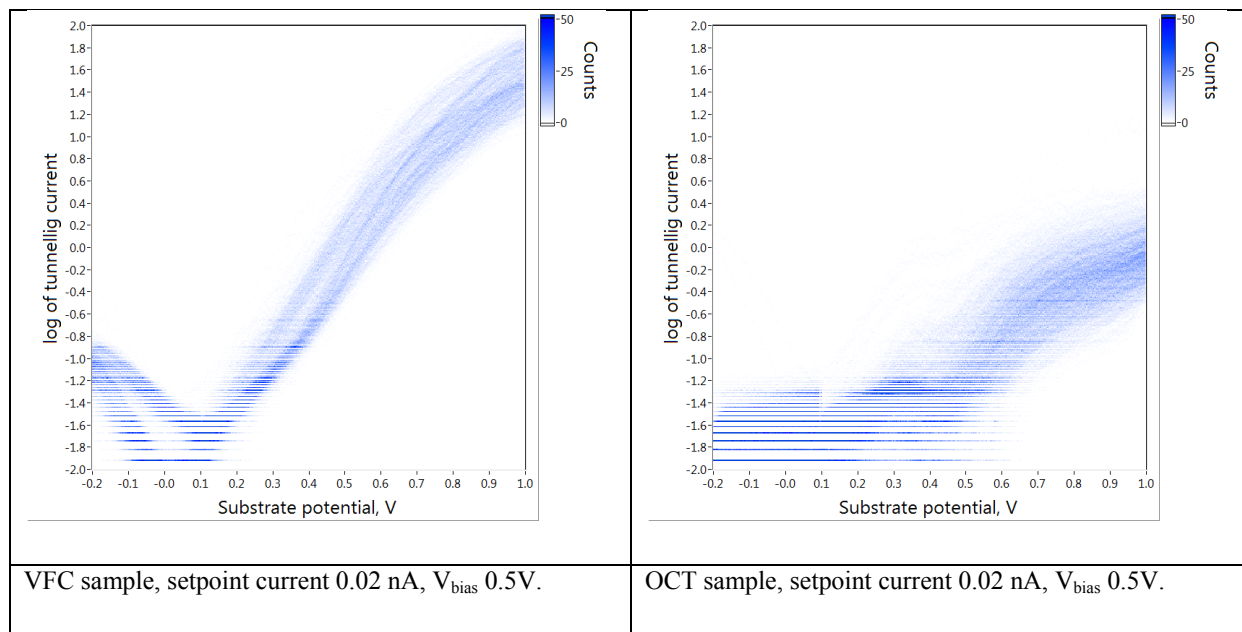


Fig. S5: Typical STM images in electrochemical conditions for OCT (a) and VFC (b) samples.

5. *In situ* scanning tunnelling spectroscopy (STS)

After the successful characterization of the samples by cyclic voltammetry, AFM and *in situ* STM, *in situ* STS measurements were carried out employing “electrolyte gating”.³ The potentials of both working electrodes (modified Si substrate and coated gold tip) were swept simultaneously (with a constant bias voltage V_{bias} between them). The data were collected automatically with a lab-written Visual Basic Script, which controlled the STM setup. The tip was repositioned after each 50 sweeps to a new area to ensure a better statistics. Usually around 500 spectra were recorded for each set of conditions. The data are presented as 2D histograms, which were constructed based on a self-written LabVIEW program. The following algorithm was applied: individual IV traces were first binned in 2D space (usually 500×500 bins) and the resulting individual 2D histograms were summed up. The results, plotted as intensity graphs, represent statistically significant *in situ* STS data.

Fig. S6 shows typical STS data sets for VFC and OCT samples as obtained at different tip-substrate separations. The latter was adjusted by the setpoint current. Clearly, increasing the setpoint current leads to a high tunnelling response upon sweeping E_s .



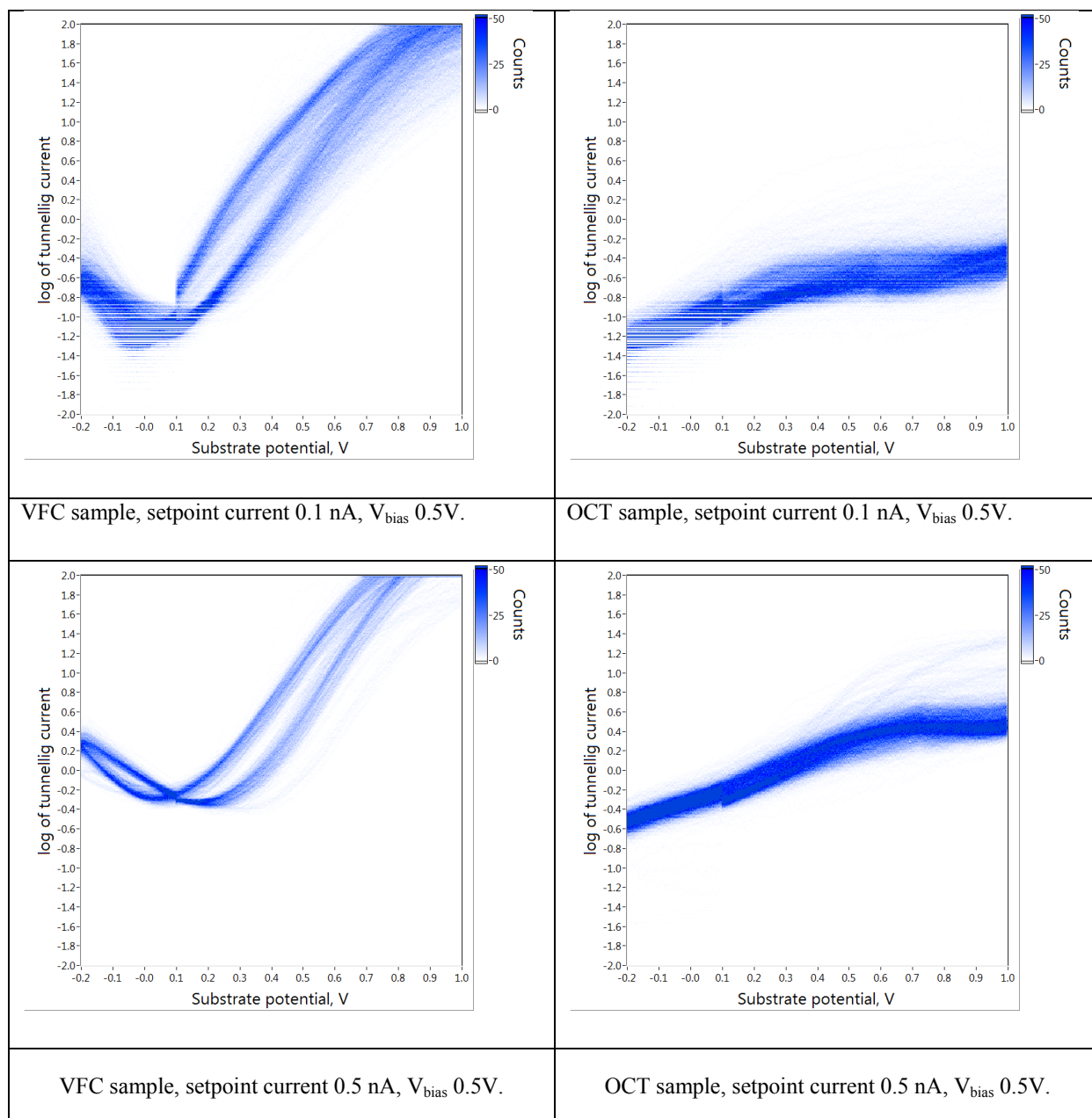


Fig. S6: Typical STS data sets for VFC and OCT samples as obtained at different setpoint currents.

References:

1. S.N. Patole, A.R. Pike, B.A. Connolly, B.R. Horrocks and A. Houlton, *Langmuir* 2003, 19, 5457.
2. L. H. Lie, S. N. Patole, A. R. Pike, L. C. Ryder, B. A. Connolly, A. D. Ward, E. M. Tuite, A. Houlton and B. R. Horrocks, *Faraday Discuss.*, 2004, 125, 235.
3. I.V. Pobelov, Z. Li and Th. Wandlowski, *J. Am. Chem. Soc.*, 2008, 130, 16045.
4. Z. Li, Th. Wandlowski, *J. Phys. Chem. C*, 2009, 113, 7821.
5. E. Laviron, *J. Electroanal. Chem. Interfacial Electrochem.*, 1979, 101, 19.
6. F. Hauquier, J. Ghilane, B. Fabre and P. Hapiot, *J. Am. Chem. Soc.*, 2008, 130, 2748.

7. B. Fabre, *Acc. Chem. Res.*, 2010, 43, 1509.
8. N. Tajimi, H. Sano, K. Murase, K.-H. Lee and H. Sugimura, *Langmuir*, 2007, 23, 3193.